

Infinite magneto-resistance and bipolar effect in spin valves driven by spin batteries

Khuôn-Việt Pham

Université Paris-Saclay, CNRS, Laboratoire de Physique des Solides, 91405 Orsay, France

khuon-viet.pham@universite-paris-saclay.fr

Abstract

It is shown that spin valves under suitable symmetry conditions exhibit an ON-OFF response to a spin battery. While a spin valve driven by a charge battery displays the usual GMR (Giant Magneto-Resistance), a pure spin current or pure spin accumulation can generate an infinite magneto-resistance effect (IMR). In practice the effect is curtailed by asymmetry but the achievable magneto-resistance ratio is still predicted to be unusually large in several example setups. It is closely related to the bipolar effect (BE) of Johnson transistor which can be triggered under the same symmetry conditions.

Contents

1	Introduction	1
2	Response function, BE & IMR.	5
2.1	Trans-resistance.	5
2.2	Bipolar effect (BE).	5
2.3	IMR.	5
3	Example setups.	6
3.1	Twin setup with shared spin battery.	6
3.2	Twins with individual spin batteries.	7
3.3	Symmetric CPP spin valves operated by two spin batteries. Parallel IMR.	7
3.4	Anti-parallel IMR in CPP MTJ & FNF trilayer.	8
4	Conclusion.	10
	References	10

1 Introduction

This paper introduces a new magneto-resistive effect, the infinite magneto-resistance (IMR) related to the giant magneto-resistance spin valve (GMR [1,2]) and to the bipolar spin transistor (BST) of Johnson [3,4].

The IMR does not rely on specific materials such as half-metals to increase GMR (Heusler alloys as in [5]) or coherent tunneling through MgO barriers [6, 7]. It consists in achieving a zero signal for a system with 2 magnetically active parts (like two ferromagnetic layers in a spin valve) so that the optimistic (resp. pessimistic) MR ratio tends to infinity (resp. unity), hence the naming of the effect as IMR. Its main characteristics are: (1) the use of a spin battery instead of a charge battery; (2) the reliance on symmetry to get rid of the offsets preventing a bipolar response in Johnson BST; (3) the reliance on Johnson-Silsbee charge-spin coupling [8] to measure the effect. Of course, the effect is curtailed by asymmetries which always exist so that the MR ratio can never be infinite and it will be one of the objectives of the paper to quantify to impact of slight asymmetries and show that the MR ratio can still be very large.

The starting point of our proposed effect is the BST. In the latter, one has a spin valve like structure $F1-N-F2$ with two collinear ferromagnets $F1$ and $F2$ connected by a paramagnetic metal N . A charge current flows through the first ferromagnet $F1$ but NOT through the second $F2$. Thanks to spin injection it induces a spin current and spin accumulation which spill into the second ferromagnet $F2$. The spin accumulation in $F2$ is detected as a charge voltage through Johnson-Silsbee charge spin coupling. It was predicted that the signal would be bipolar as a function of the magnetization polarization (up or down): $V_c \propto \text{sgn}(M_z) \propto \pm V_1$. Experimentally the bipolarity has proved elusive to detect and one observes instead

$$V_c = V_0 + V_1 \sigma \quad (1)$$

(where $\sigma = \pm$) with a **voltage offset** V_0 [3, 9–16]. The origin of these offsets have been credited to various causes such as current inhomogeneities [11], heating [14–16], departures from one dimensional geometry [9].

Conceptually one can deconstruct the BST into three components: (1) a spin battery, made up of the ferromagnet $F1$ when a charge current flows through it; (2) a load $F2$ for the spin current and spin accumulation created by the spin battery; (3) a charge (voltage or current) measurement apparatus.

The systems we consider will be driven by a spin battery like the original BST but differ in that the load is not a single ferromagnet but has at least two magnetically active regions. For instance for collinear systems, we will have in general a voltage response

$$V_c = V_0 + V_1 \sigma_1 + V_2 \sigma_2 + V_{12} \sigma_1 \sigma_2 \quad (2)$$

where $\sigma_{1/2} = \pm$ track the magnetization directions. The voltage offsets come from V_0 and V_{12} . But should they vanish due to some symmetry, one would then have

$$V_c = V_1 \sigma_1 + V_2 \sigma_2 \quad (3)$$

exhibiting a bipolar response when both magnetizations are switched ($\sigma_{1/2} \rightarrow -\sigma_{1/2}$). Suppose now that due to a stronger symmetry $V_1 = V_2$ (resp. $V_1 = -V_2$); V_c will then obviously vanish whenever the two magnetizations are antiparallel (resp. parallel). This implies that the optimistic MR ratio $(V_{HIGH} - V_{LOW})/V_{LOW}$ will be infinite. This is the IMR which the main topic of this paper. In such a spin valve, a single magnetization needs to be switched; if instead both are switched, one recovers a BE.

Aside from symmetry, the other main ingredient is the use of a spin battery instead of a regular charge battery. The reason is that oftentimes the response $r_c(\sigma) = \partial V_c / I_c$ is even in σ (the magnetization direction), $r_c(-\sigma) = r_c(\sigma)$ which implies that $V_1 = 0$ so that the IMR is not possible with a pure charge battery (since it lacks any magnetically active region). In contrast a spin battery will induce an odd term in the voltage response, which is required for the BE and IMR.

The third ingredient is the reliance on Johnson-Silsbee charge-spin coupling (the coupling of charge and spin transport in magnetic systems) to get a (charge) voltage or current reading

from magnetic changes. The advantage of a voltage measurement over a current one is that it avoids Joule heating. But theoretically either one could be done.

What is of paramount importance is to have symmetrical setups which will allow to get rid by construction of any offsets. A simple recipe is to have two copies of the same system as in Fig. 1-a: the offsets obviously cancel out. This is an example of what we will christen as 'twin systems'.

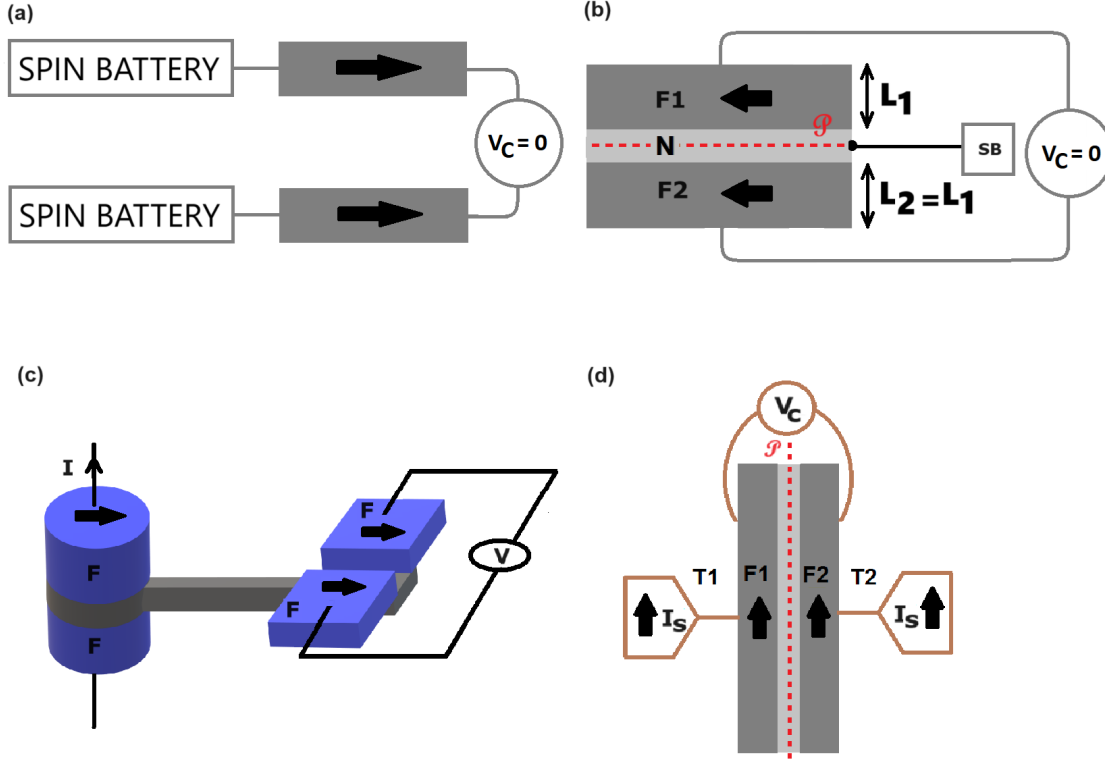


Figure 1: (a) The voltage measured across two copies of the same system (and batteries) vanishes by symmetry. (b) FNF valve connected to a spin battery and a voltmeter. If the combined system is symmetrical under left-right exchange, then the voltage must vanish by symmetry. The layers can be viewed as parallel to the figure plane (as in non-local geometries) or to be perpendicular. SB: spin battery. (c) Same as (b) but depicted with an FNF nanopillar playing the role of the SB. (d) CPP trilayer driven symmetrically by two spin batteries. For parallel magnetizations, the voltage again vanishes (for symmetric probes). The black arrows depict the magnetization directions.

Another example of a 'twin system' is given in Fig. 1-b. It is an *FNF* valve in a non-local geometry with identical ferromagnets and layers parallel to the figure plane; it could also be considered to be a trilayer with layers perpendicular to the figure plane. A spin battery injects a spin current through the intermediate *N* layer. The charge voltage across the trilayer obviously vanishes when the ferromagnets have parallel magnetizations but is non-zero for anti-parallel ones. In practice the vanishing of the signal is constrained by the degree of symmetry. Suppose for instance that the widths of the ferromagnets are equal to $l_m \pm \delta l$. Then we expect a scaling:

$$\frac{V_c^{AP} - V_c^P}{V_c^P} \sim \frac{l_m}{\delta l} \quad (4)$$

so for widths equal with an accuracy of 1%, the ratio reaches $10^2 = 10^4\%$. Other geometrical

asymmetries will of course affect this rough estimate. For the same twin setup, the BE is achieved by starting from an antiparallel configuration and flipping both magnetizations.

There is a wide variety of spin batteries currently in use and among others: spin injection devices (a charge current gets polarized by traversing a ferromagnet [17–19]); spin Hall devices (a transverse spin current is generated when there is a longitudinal charge current due to spin-orbit interactions [20]); spin pumps (a rotating bulk magnetization engenders a spin current, as in the ferromagnetic resonance battery [21, 22]); tunnel junctions relying on photoexcitation (circularly polarized light at FM/semiconductor tunnel junctions excites spin polarized carriers [23]); devices relying on the spin Seebeck effect (a thermal gradient can generate a spin current) [24, 25]. Fig. 1-c shows the twin system from Fig. 1-b with an FNF nanopillar acting as a spin battery.

There are other possible setups than 'twin setups' which will exhibit IMR and bipolarity, as a result of symmetry. For instance consider a CPP symmetric trilayer where instead of a charge battery, one connects the layers to two spin batteries as in Fig. 1-d. (The CPP qualifier, current perpendicular to plane, comes from the fact that if one replaced the voltage probes by current ones, the charge current would be perpendicular to the layers.) This setup exhibits IMR for identical incoming spin currents and parallel magnetizations. We will discuss later a similar setup with opposite spin currents; one then has IMR for antiparallel magnetizations.

The latter case is actually easy to understand in terms of a resistor analogy. We consider a spin current source in a two-channel model (Fig. 2) : this is tantamount to having opposite charge current sources for each spin channel. In the resistor analogy for a CPP symmetric spin valve with anti-parallel magnetizations *driven by a charge battery*, the currents flowing in each spin channel would be equal $I_{\uparrow} = I_{\downarrow}$ and the voltages for each spin channel would be identical in the anti-parallel case $V_{\uparrow} = V_{\downarrow}$. In the antiparallel case for a spin current source driving the resistors (Fig.2-(b)), since the currents are opposite $I_{\uparrow} = -I_{\downarrow} = I_s/2$, the channel voltages are also opposite $V_{\uparrow} = -V_{\downarrow}$ so that $V_c = 0$. The charge voltage divided by the spin current has the dimension of a resistance $R = V_c/I_s$. The corresponding MR ratio $(R^{AP} - R^P)/R^{AP}$ goes to infinity (IMR effect).

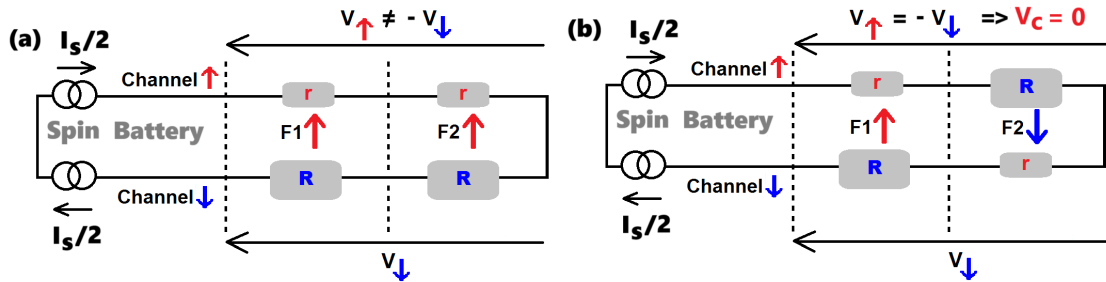


Figure 2: Resistor model of a spin valve driven by a spin current source. The charge voltage is $V_c = (V_{\uparrow} + V_{\downarrow})/2$. (a) $V_c \neq 0$ when ferromagnets $F1$ and $F2$ have parallel magnetizations. (b) But for anti-parallel magnetizations, the voltage V_c obviously vanishes since $V_{\uparrow} = (r + R) I_s/2 = -V_{\downarrow}$.

2 Response function, BE & IMR.

2.1 Trans-resistance.

Let us define a charge-spin trans-resistance encoding the response to a spin battery:

$$r_{cs} = \left(\frac{\partial V_c}{\partial I_s} \right)_{I_c=0}, \quad (5)$$

where the spin current is defined in electrical units as $I_s = I_\uparrow - I_\downarrow$ for collinear setups. It has the dimension of a resistance. The basic geometries we consider are therefore 3 terminal ones, two terminals used for the voltage measurement and one terminal connected to the spin battery. We will make the hypothesis that the spin battery is a perfect spin current source which outputs a constant spin current I_s , whatever the load it is attached to. This is not a very stringent condition. It is easy to take into account spin backflow into the battery through the internal spin resistance concept [26], which in practice will translate into a reduced response. Let us suppose that the load comprises $N = 2$ magnetically active regions, whose **magnetizations are collinear (but maybe have different directions)** and can be controlled independently. One can write therefore: $r_{cs} = r_{cs}(\sigma_1, \sigma_2)$ where $\{\sigma_1 = \pm 1, \sigma_2 = \pm 1\}$ index the magnetizations of the 2 regions relative to a given quantization axis. r_{cs} is simply a multilinear polynomial in σ_1 and σ_2 :

$$r_{cs}(\sigma_1, \sigma_2) = r_0 + r_1 \sigma_1 + r_2 \sigma_2 + r_{12} \sigma_1 \sigma_2. \quad (6)$$

The resistance r_{cs} can take four independent values.

2.2 Bipolar effect (BE).

This requires the concurrent switching of both magnetizations. One has a bipolar effect if for some values of σ_1 and σ_2

$$r_{cs}(-\sigma_1, -\sigma_2) = -r_{cs}(\sigma_1, \sigma_2); \quad (7)$$

which implies that $r_0 = -r_{12} \sigma_1 \sigma_2$. In the special case $r_0 = 0$, $r_{12} = 0$, the bipolarity will occur for any values of σ_1 and σ_2 . The twin system of Fig.1-a obeys

$$r_{cs}(\sigma_2, \sigma_1) = -r_{cs}(\sigma_1, \sigma_2) \quad (8)$$

so that $r_0 = 0$, $r_{12} = 0, r_1 = -r_2$. For Fig. 1-b, eq.(8) is also true since a symmetry through plane (\mathcal{P}) parallel to the layers and perpendicular to the Figure maps each ferromagnetic layer unto the other but leaves the spin battery invariant. But the voltage probes are exchanged across that plane so that $V_c \rightarrow -V_c$. It follows that: $r_{cs}(\sigma_1, \sigma_2) = r_1 \cdot (\sigma_1 - \sigma_2)$. If one starts from an antiparallel configuration and swaps both magnetizations, one therefore has a bipolar response:

$$r_{cs}(\sigma_1, -\sigma_1) = 2r_1 \sigma_1 = -r_{cs}(-\sigma_1, \sigma_1). \quad (9)$$

2.3 IMR.

For the twin system of Fig.1-a & b, it also follows from eq.(8) that $r_{cs}^P = r_{cs}(\sigma_1, \sigma_1) = 0$ while $r_{cs}^{AP} \neq 0$. We have a **parallel IMR**. The pessimistic MR ratio is 100% and the optimistic MR ratio is infinite. If one starts from an antiparallel setup and one switches a single magnetization, the response vanishes (IMR). A similar symmetry condition can not be enforced when there is a single $N = 1$ magnetized region because in order to detect a charge voltage through Johnson-Silsbee charge-spin coupling, the measurement probes must be positioned asymmetrically.

Since the condition for IMR also allows the BE, let us compare the two effects for the setups of Fig. 1-a, 1-b. IMR is observed by switching a single magnetization while bipolarity

requires switching two magnetizations, which may or may not be possible or desirable in a given setup. The amplitude of the IMR effect is $|r_{cs}^{AP} - r_{cs}^P| = 2r_1$, while the bipolar effect has an amplitude which is twice as large. There is therefore a trade-off between the two effects: IMR is smaller but easier to observe, requiring a single magnetization to be switched, while bipolarity has the larger signal but requires both magnetizations to be switched.

Let us compare with the regular charge resistance $r_c = \left(\frac{\partial V_c}{\partial I_c}\right)$; the latter has a similar dependence in general. But if the system is invariant when both magnetizations are reversed, one has the simpler dependence: $r_c(\sigma_1, \sigma_2) = r_{c0} + r_{c12} \sigma_1 \sigma_2$. One recovers the usual GMR for a spin valve subjected to a charge battery. An infinite MR ratio is much more difficult to engineer. For instance, let us consider Juilliére model for TMR. Then: $r_c \propto (1 + P_1 P_2)$ where $P_{1/2}$ is a DOS spin polarization. For identical layers, $|P_1| = |P_2| = P$. An infinite MR ratio would then require $(1 - P^2) = 0$, that is $P = 1$ or a half-metal. This is a very stringent condition when compared with the IMR discussed above.

In GMR spin valves, one usually anchors one of the two ferromagnets so that a single ferromagnet can be switched under normal operating conditions. Doing so here would obviously prevent the symmetries enabling the IMR and bipolar effects. This is another difference with conventional GMR spin valves. The switching field needs to be tailored according to the effect one wishes to trigger, whether it be IMR or the bipolar effect.

3 Example setups.

3.1 Twin setup with shared spin battery.

To quantify the impact of asymmetries, one can make explicit calculations for the geometry of Fig.(1-b) in the one dimensional limit, using Valet-Fert drift diffusion model. We introduce P_{F1} and P_{F2} are the conductivity polarizations for ferromagnets 1 & 2, contact resistance r_c , conductance polarization P_{c1} and P_{c2} at the interfaces between the ferromagnets 1 & 2 and the central paramagnetic layer, contact resistances r'_c , conductance polarization P'_{c1} and P'_{c2} at the interfaces between the ferromagnets 1 & 2 and the measurement leads. We also define $l_{1/2}$ the ferromagnet layer widths relative to l_F the spin relaxation length of the ferromagnets. Defining $l_m = \frac{l_1+l_2}{2}$, $\delta l = \frac{l_1-l_2}{2}$ as well as $\sinh_m = \sinh l_m$, $\cosh_m = \cosh l_m$,

$$X = \frac{r_N + r'_c}{r_F}, f_m = \frac{\sinh_m + X \cosh_m}{\cosh_m + X \sinh_m}, \quad (10)$$

one finds after tedious calculations that r_{cs} splits into 3 parts, a bulk contribution (I) and two interfacial ones (II & III):

$$r_{cs}^I = (P_{F1} - P_{F2}) [-f_m (\cosh_m - 1) + \sinh_m] \frac{r_F}{2} + \delta l (P_{F1} + P_{F2}) \frac{r_F}{2} \alpha, \quad (11)$$

$$r_{cs}^{II} = (P_{c1} - P_{c2}) \frac{r_c}{2} + \delta l (P_{c1} + P_{c2}) \frac{r_c}{2} \beta, \quad (12)$$

where α and β are factors which depend on the geometry and the various spin resistances (for their exact expressions, we refer to [27]).

$$r_{cs}^{III} = (P'_{c1} - P'_{c2}) \frac{r'_c}{2} (\cosh_m - f_m \sinh_m) + \delta l (P'_{c1} + P'_{c2}) \frac{r'_c}{2} (\cosh_m - f_m \sinh_m) \quad (13)$$

One can compute a resistance ratio as $MR = \frac{R_{AP} - R_P}{R_P}$ where the subscripts P/AP refer to parallel or anti-parallel magnetizations; it follows that:

$$R_P = o(\delta l), \quad MR \propto \delta l^{-1} \quad (14)$$

Asymmetries in transverse directions should in principle be taken into account so that most generally one expects

$$MR \propto \left(\sum_{i=x,y,z} C_i \frac{\delta l_i}{l_i} \right)^{-1} \quad (15)$$

but for thin films, the dominant contribution will come from the width so that other asymmetries can be neglected. As an illustration, consider a Co-Cu-Co trilayer. For all the following figures, we refer to [28]; Piraux et al find at 77 K that $l_F = 36 \text{ nm}$. MSU Reilly et al have data consistent with a large l_F maybe larger than 60 nm at 4.2 K. If the widths are about $10 \pm 0.5 \text{ nm}$, $\delta l \sim \frac{1}{60}$ so up to numerical factors $MR \sim 6000\%$.

It is also important to have an idea of the range of the HIGH signal. Let's use MSU results for CoCu at 4.2 K and for simplicity assume that $P_c \sim P'_c = 0.77 \pm 0.05$, $P_F = 0.46 \pm 0.05$, $2r_c A \sim 2r'_c A = 1.02 \pm 0.04 f\Omega m^2$, $t_{Co} = 2 - 10 \text{ nm}$, $l_{Co} > 60 \text{ nm}$ and $\rho_F(Co) = 75 \pm 5 \text{ n}\Omega m$, $\rho_N(Cu) = 6 \pm 1 \text{ n}\Omega m$. Then $X \sim 1$, $f_m \sim 1$. So for AP ferromagnets:

$$r_{cs}^{high} A \sim 1 f\Omega m^2. \quad (16)$$

This will be in the range of $R = 1 \Omega$ for $A = 10^{-3} \mu m^2$ which corresponds to a nanopillar.

3.2 Twins with individual spin batteries.

We consider two identical systems connected to a spin battery and interconnected by voltage probes (Fig.(1-a)). This geometry is better suited to the observation of IMR than the previous one because it is easier to switch a single ferromagnet since they can be well separated spatially. One must take into account spin batteries asymmetry δI_s ; one finds a MR ratio

$$R_p = \circ(\delta l) + \circ(\delta I_s), \quad MR \propto \left(\frac{\delta l}{l} + C \frac{\delta I_s}{I_s} \right)^{-1}. \quad (17)$$

For very wide ferromagnets, it can be shown that it is better to have $X = \frac{r_N + r'_c}{r_F} \sim 1$ so that $C \sim 1 - 2$. In the opposite limite of very thin ferromagnets, $C \propto X$, the MR ratio will be boosted by transparent contacts ($r'_c \ll (r_N, r_F)$) which lower C . For very resistive contacts such that $(r'_c, r_c) \gg (r_N, r_F)$ and $X \gg 1$, one finds that $C \propto 1/X$ provided the ferromagnets are not too thin. The reason for this potential enhancement is that the resistive contacts hinder the backflow of spin accumulation and allow its build-up. But the spin current asymmetry will likely limit any such improvement. The HIGH signal is dominated by interfaces in the limit of very thin ferromagnets: $r_{cs}^{high} \rightarrow 2 \{P_c r_c + P'_c r'_c\}$ while for very thick layers: $r_{cs}^{high} \rightarrow 2 \{P_c r_c + P_F r_F\}$. Using the same parameters as above, one finds again a range $r_{cs}^{high} A \sim 1 f\Omega m^2$.

3.3 Symmetric CPP spin valves operated by two spin batteries. Parallel IMR.

One can define new transport coefficients per:

$$V_c = r_{cs}^L I_{s,L} + r_{cs}^R I_{s,R}. \quad (18)$$

Since there is a new control parameter, it is easy to get a zero response (IMR) by adjusting one spin current relative to the other. One can then sweep the value of, say, the spin current $I_{s,L}$ until $I_{s,L} = -\frac{r_{cs}^R I_{s,R}}{r_{cs}^L}$. **No symmetry is required** but the trade-off is that (1) the system is larger since there are two spin batteries, (2) while an adjustment is easy to do in a lab context, it is much less convenient to do so in industrial applications.

It is therefore advantageous to engineer symmetrical systems which can have reproducible behaviours. Consider for instance Fig.1-d which shows a spin valve in a CPP geometry (if the voltmeter was shorted, a charge current would flow in a direction orthogonal to the layers). **Note that the setup in Fig. 1-d could represent also a nano-pillar or a non-local geometry in addition to the usual multi-layer thin films.** The spin current from the batteries are oriented to be **incoming in the load** (outgoing from the batteries). If the ferromagnetic layers and the spin batteries are identical, there is a plane of symmetry \mathcal{P} in the paramagnetic layer parallel to the layers. Obviously $V_c = 0$ when the magnetizations are parallel. One has a **parallel IMR**. If one starts with antiparallel magnetizations and switches both of them, one gets a bipolar effect.

After rotating the setup around an axis in the middle of the paramagnetic layer:

$$V_c \longrightarrow -V_c, I_{s,L} \longrightarrow I_{s,R}, (\sigma_1, \sigma_2) \longrightarrow (\sigma_2, \sigma_1). \quad (19)$$

Therefore:

$$V_c = r_{cs}^L(\sigma_1, \sigma_2) I_{s,L} + r_{cs}^R(\sigma_1, \sigma_2) I_{s,R}, \quad (20)$$

$$-V_c = r_{cs}^L(\sigma_2, \sigma_1) I_{s,R} + r_{cs}^R(\sigma_2, \sigma_1) I_{s,L}, \quad (21)$$

which implies

$$r_{cs}^L(\sigma_1, \sigma_2) = -r_{cs}^R(\sigma_2, \sigma_1). \quad (22)$$

Therefore for identical currents $I_{s,L} = I_{s,R} = I_s$

$$V_c = [r_{cs}^L(\sigma_1, \sigma_2) - r_{cs}^L(\sigma_2, \sigma_1)] I_s \quad (23)$$

which is antisymmetric under exchange of the magnetizations, $V_c(\sigma_2, \sigma_1) = -V_c(\sigma_1, \sigma_2)$. This implies a **parallel IMR** or vanishing response for parallel magnetizations:

$$V_c(\sigma_1, \sigma_1) = -V_c(\sigma_1, \sigma_1) = 0 \quad (24)$$

and a bipolar effect for antiparallel magnetizations when flipping both of them for identical currents: $V_c(\sigma_1, -\sigma_1) = -V_c(-\sigma_1, \sigma_1)$. Detailed calculations on an FNF trilayer exhibiting such a parallel IMR are given elsewhere [27]. In the limit of infinite ferromagnets, one finds

$$MR = \frac{V_c^{AP} - V_c^P}{V_c^P} \sim \frac{I_{s,0}^m}{\delta I_s} \quad (25)$$

3.4 Anti-parallel IMR in CPP MTJ & FNF trilayer.

It is also possible to engineer an **anti-parallel IMR**. Fig.3-a shows such a setup. A CPP trilayer is connected symmetrically to two spin batteries which inject opposite spin currents. If the voltage probes are also symmetrical, the charge voltage must vanish as shown in Fig.3. Indeed let us rotate the setup by an angle π around an axis \mathcal{P} in the middle of the layers (Fig.3-d): this exchanges the spin batteries and the ferromagnets and the voltage drop gets reversed $V_c \longrightarrow -V_c$. But one could also rotate the setup by an angle π around an axis \mathcal{F} splitting the layers symmetrically (Fig.3-b): all the magnetizations get reversed; the spin current reference axis is also reversed but the charge voltage is obviously unchanged. But a spin current $+I_s$ against a given magnetization reference axis \mathbf{M} is equivalent to a spin current $-I_s$ with a reversed reference axis $-\mathbf{M}$. One therefore ends up with Fig.3-c which is equivalent to Fig.3-d apart from an opposite voltage. This implies that $V_c = 0$. The obvious issue with such a setup is that both the spin batteries and the voltage probes must be located at the same positions. This

is however easy to relax by doubling the voltage probes and positioning them in a symmetric manner with respect to symmetry plane \mathcal{F} (see Fig.3-e); one would then measure two voltage drops V_{c1} and V_{c2} which might not be offset-free but their average will be: $V_c = (V_{c1} + V_{c2})/2$.

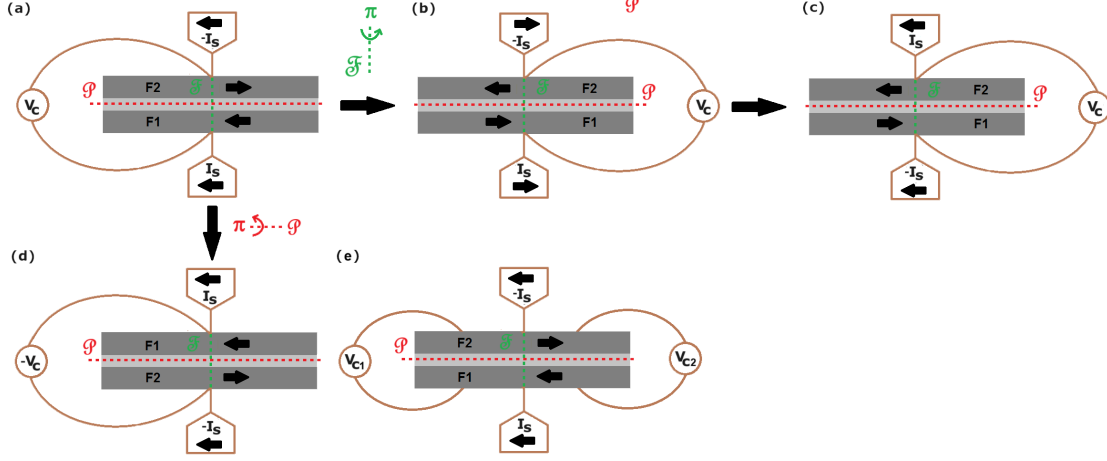


Figure 3: (a) CPP symmetric spin valve connected to two spin batteries injecting opposite spin currents I_s into the ferromagnets. The black arrows show the magnetization direction in each layer ($F1$ or $F2$) or the reference direction used to measure the spin current (in the spin batteries). (b) Setup rotated around a symmetry axis \mathcal{D} assumed to exist. (b) Previous setup where the spin currents take opposite values if the reference axis is flipped in the spin batteries. (d) Setup rotated by an angle π around a symmetry axis \mathcal{P} assumed to exist in the middle. Comparing (c) and (d) shows they're identical setups provided the ferromagnets $F1$ & $F2$ are identical (for symmetrical voltage probes), so that for anti-parallel magnetization, there is no voltage drop across terminals T_1 and T_2 . (e) Instead of two voltage probes in the middle of the layers, it might be easier to use 2 sets of voltage probes positioned symmetrically with respect to axis \mathcal{F} .

We illustrate such an AP-IMR with an MTJ (magnetic tunnel junction). The junction voltage can be shown using Julliere model [17] and Slonczewski circuit theory [29] to be:

$$V_J = -\frac{1}{g_0} \frac{P_1 + P_2}{(1 - P^2)^2} I_{s,J} \quad (26)$$

where $P_{1/2}$ are the usual DOS polarizations, $P = |P_{1/2}|$, $g_0 = \Gamma n_1 n_2$ (with Γ the tunneling probability, $n_{1/2}$ the total density of states) and $I_{s,J}$ the spin current across the junction. This obviously vanishes for antiparallel magnetizations which implies an **anti-parallel IMR**. This calculation neglects however the spin accumulation effects in the ferromagnets. For very thin ferromagnets, a more complete calculation incorporating the spin accumulation in the ferromagnets, leads to

$$TMR = \frac{V_c^P - V_c^{AP}}{V_c^{AP}} \sim \frac{P_c r_c}{P_F r_F \delta l} \quad (27)$$

where $P_c r_c = \frac{1}{g_0} \frac{2P}{(1-P^2)^2}$; P_F is the conductivity polarization of the ferromagnets and r_F is their usual spin resistance; $\delta l = (d_1 - d_2)/l_F$ is the difference in widths of the ferromagnets measured against the spin relaxation length. Let us put some figures into it. For instance the DOS polarization for Co is $P_1 = P_{Co} \sim 0.34$ at room temperature in Moodera and coll. [30] so that $P_c = \frac{P_1 + P_2}{1 + P^2} = 0.61$; we also take $P_F(\text{Co}) \sim 0.5$ (see for instance Ref. [31]) and the

ratio $r_c/r_F > 10^4 - 10^5$. If we assume $l_F(Co) \sim 40 \text{ nm}$ as in Table 3 of Ref. [32] and that the ferromagnet widths are equal up to a monolayer, $\delta l \sim 0.1 \text{ nm}/40 \text{ nm} \sim 2.5 \cdot 10^{-2}$, then $TMR \sim 10^5 - 10^7 = 10^7 - 10^9\%$. The case of very thin layers is the optimal one in terms of TMR ratio.

Let us consider layers which are not infinitely thin; for instance, we assume equal widths $d_1 = d_2 = 5 \text{ nm}$ up to a monolayer; this means $l_{1/2} = d_{1/2}/l_F = 0.125$. Using the same figures as above numbers, a more realistic calculation [27] shows that the spin current asymmetry can usually be neglected and leads to $TMR \sim 10^5\%$, which is still extremely large.

For an FNF trilayer in the same geometry, in the limit of thin layers, one gets a similar MR ratio. The ratio is however much higher for an MTJ because r_c is considerably larger by a factor $10^3 - 10^5$. For all metallic spin valves, a spin battery based on ferromagnetic resonance would be able to achieve HIGH signals in the $1 - 100 \mu\text{V}$ range. By using an MTJ, since the resistance is multiplied by a factor $10^3 - 10^5$, this implies that $m\text{V}$ signals are very achievable which would make such a spin battery driven MTJ quite useable.

What would be the impact of MgO barriers? This would increase the value of P_c and the TMR ratio. But it is not as critical as having very small widths for the ferromagnets as well as a very small width asymmetry. For instance, let us consider figures extracted from Yuasa and coll. [33]. $RA \sim 10 - 10^7 \Omega\mu\text{m}^2$ and the TRM ratio reaches 180% so $P_1 = 0.69$ or $P_c = 0.93$. If we plug this in the previous TMR ratio calculation, this would increase it by a factor 1.5 which is nice but not as crucial as having a very small δl .

4 Conclusion.

We have introduced several spin valve setups which due to symmetry can exhibit both the bipolar effect of Johnson spin transistor and an IMR. An obvious application of IMR and BE would be more sensitive magnetic sensors so an experimental confirmation of these predictions would be very useful. An essential component for the occurrence of both BE and IMR is to replace charge batteries by spin batteries since this allows the occurrence in response functions of odd terms $\propto \text{sgn}(M_x)$. Since real systems are never perfectly symmetric, we have also quantified the impact of length & spin current asymmetries. The MR ratio can still reach high ranges $10 - 10^3$. The simplest system to observe the BE is the twin system with shared spin battery; for observation of IMR, it is better to test on a twin system with independent spin batteries. The CPP MTJ with two spin batteries is quite promising in comparison with the CPP FNF trilayer due to the much larger HIGH signal which should make the $m\text{V}$ range quite reachable. Extensions of this work to non-collinear systems with symmetries, to CIP setups, to parallel IMR in CPP systems and inclusion of non-ideal spin batteries are discussed elsewhere [27].

References

- [1] B. Dieny, V. S. Speriosu, S. S. P. Parkin, B. A. Gurney, D. R. Wilhoit and D. Mauri, *Giant magnetoresistive in soft ferromagnetic multilayers*, Physical Review B **43**(1), 1297 (1991), doi:[10.1103/PhysRevB.43.1297](https://doi.org/10.1103/PhysRevB.43.1297).
- [2] C. Chappert, A. Fert and F. N. Van Dau, *The emergence of spin electronics in data storage*, Nat Mater **6**(11), 813 (2007), doi:[10.1038/nmat2024](https://doi.org/10.1038/nmat2024).
- [3] M. Johnson, *Bipolar Spin Switch*, Science **260**(5106), 320 (1993), doi:[10.1126/science.260.5106.320](https://doi.org/10.1126/science.260.5106.320).

- [4] M. Johnson, *Spin accumulation in gold films*, Physical Review Letters **70**(14), 2142 (1993), doi:[10.1103/PhysRevLett.70.2142](https://doi.org/10.1103/PhysRevLett.70.2142).
- [5] T. Kimura, N. Hashimoto, S. Yamada, M. Miyao and K. Hamaya, *Room-temperature generation of giant pure spin currents using epitaxial Co₂FeSi spin injectors*, NPG Asia Materials **4**(3), e9 (2012), doi:[10.1038/am.2012.16](https://doi.org/10.1038/am.2012.16), Number: 3 Publisher: Nature Publishing Group.
- [6] J. Mathon and A. Umerski, *Theory of tunneling magnetoresistance of an epitaxial Fe/MgO/Fe(001) junction*, Physical Review B **63**(22), 220403 (2001), doi:[10.1103/PhysRevB.63.220403](https://doi.org/10.1103/PhysRevB.63.220403), Publisher: American Physical Society.
- [7] W. H. Butler, X.-G. Zhang, T. C. Schulthess and J. M. MacLaren, *Spin-dependent tunneling conductance of $\text{Fe}|\text{MgO}|\text{Fe}$ sandwiches*, Physical Review B **63**(5), 054416 (2001), doi:[10.1103/PhysRevB.63.054416](https://doi.org/10.1103/PhysRevB.63.054416), Publisher: American Physical Society.
- [8] M. Johnson and R. H. Silsbee, *Coupling of electronic charge and spin at a ferromagnetic-paramagnetic metal interface*, Physical Review B **37**(10), 5312 (1988), doi:[10.1103/PhysRevB.37.5312](https://doi.org/10.1103/PhysRevB.37.5312).
- [9] M. Johnson and R. H. Silsbee, *Calculation of nonlocal baseline resistance in a quasi-one-dimensional wire*, Physical Review B **76**(15), 153107 (2007), doi:[10.1103/PhysRevB.76.153107](https://doi.org/10.1103/PhysRevB.76.153107).
- [10] A. Fert, J. M. George, H. Jaffres and R. Mattana, *Semiconductors Between Spin-Polarized Sources and Drains*, IEEE Transactions on Electron Devices **54**(5), 921 (2007), doi:[10.1109/TED.2007.894372](https://doi.org/10.1109/TED.2007.894372).
- [11] M. Ichimura, *Geometrical effect on spin current in magnetic nanostructures*, Journal of Applied Physics **95**, 7255 (2004), doi:[10.1063/1.1688679](https://doi.org/10.1063/1.1688679).
- [12] J. Hamrle, T. Kimura, Y. Otani, K. Tsukagoshi and Y. Aoyagi, *Current distribution inside Py/Cu lateral spin-valve devices*, Physical Review B **71**(9), 094402 (2005), doi:[10.1103/PhysRevB.71.094402](https://doi.org/10.1103/PhysRevB.71.094402).
- [13] J. Hamrle, T. Kimura, T. Yang and Y. Otani, *Three-dimensional distribution of the spin-polarized current inside nanostructures*, Journal of Applied Physics **98**(6), 064301 (2005), doi:[10.1063/1.2037868](https://doi.org/10.1063/1.2037868).
- [14] S. Garzon, I. Žutić and R. A. Webb, *Temperature-Dependent Asymmetry of the Nonlocal Spin-Injection Resistance: Evidence for Spin Nonconserving Interface Scattering*, Physical Review Letters **94**(17), 176601 (2005), doi:[10.1103/PhysRevLett.94.176601](https://doi.org/10.1103/PhysRevLett.94.176601).
- [15] F. Casanova, A. Sharoni, M. Erekhinsky and I. K. Schuller, *Control of spin injection by direct current in lateral spin valves*, Physical Review B **79**(18), 184415 (2009), doi:[10.1103/PhysRevB.79.184415](https://doi.org/10.1103/PhysRevB.79.184415).
- [16] F. L. Bakker, A. Slachter, J.-P. Adam and B. J. van Wees, *Interplay of Peltier and Seebeck Effects in Nanoscale Nonlocal Spin Valves*, Physical Review Letters **105**(13), 136601 (2010), doi:[10.1103/PhysRevLett.105.136601](https://doi.org/10.1103/PhysRevLett.105.136601).
- [17] M. Julliere, *Tunneling between ferromagnetic films*, Physics Letters A **54**(3), 225 (1975), doi:[10.1016/0375-9601\(75\)90174-7](https://doi.org/10.1016/0375-9601(75)90174-7).

- [18] M. N. Baibich, J. M. Broto, A. Fert, F. N. Van Dau, F. Petroff, P. Etienne, G. Creuzet, A. Friederich and J. Chazelas, *Giant Magnetoresistance of (001)Fe/(001)Cr Magnetic Superlattices*, Physical Review Letters **61**(21), 2472 (1988), doi:[10.1103/PhysRevLett.61.2472](https://doi.org/10.1103/PhysRevLett.61.2472).
- [19] G. Binash, P. Grünberg, F. Saurenbach and W. Zinn, *Enhanced magnetoresistance in layered magnetic structures with antiferromagnetic interlayer exchange*, Physical Review B **39**(7), 4828 (1989), doi:[10.1103/PhysRevB.39.4828](https://doi.org/10.1103/PhysRevB.39.4828).
- [20] S. O. Valenzuela and M. Tinkham, *Direct electronic measurement of the spin Hall effect*, Nature **442**(7099), 176 (2006), doi:[10.1038/nature04937](https://doi.org/10.1038/nature04937).
- [21] A. Brataas, Y. Tserkovnyak, G. E. W. Bauer and B. I. Halperin, *Spin battery operated by ferromagnetic resonance*, Physical Review B **66**(6), 060404 (2002), doi:[10.1103/PhysRevB.66.060404](https://doi.org/10.1103/PhysRevB.66.060404).
- [22] S. M. Watts, J. Grollier, C. H. van der Wal and B. J. van Wees, *Unified Description of Bulk and Interface-Enhanced Spin Pumping*, Phys. Rev. Lett. **96**(7), 077201 (2006), doi:[10.1103/PhysRevLett.96.077201](https://doi.org/10.1103/PhysRevLett.96.077201).
- [23] M. W. J. Prins, H. v. Kempen, H. v. Leuken, R. A. d. Groot, W. V. Roy and J. D. Boeck, *Spin-dependent transport in metal/semiconductor tunnel junctions*, Journal of Physics: Condensed Matter **7**(49), 9447 (1995), doi:[10.1088/0953-8984/7/49/010](https://doi.org/10.1088/0953-8984/7/49/010).
- [24] K. Uchida, S. Takahashi, K. Harii, J. Ieda, W. Koshibae, K. Ando, S. Maekawa and E. Saitoh, *Observation of the spin Seebeck effect*, Nature **455**(7214), 778 (2008), doi:[10.1038/nature07321](https://doi.org/10.1038/nature07321), Number: 7214 Publisher: Nature Publishing Group.
- [25] A. Kirihara, K. Kondo, M. Ishida, K. Ihara, Y. Iwasaki, H. Someya, A. Matsuba, K.-i. Uchida, E. Saitoh, N. Yamamoto, S. Kohmoto and T. Murakami, *Flexible heat-flow sensing sheets based on the longitudinal spin Seebeck effect using one-dimensional spin-current conducting films*, Scientific Reports **6**(1), 23114 (2016), doi:[10.1038/srep23114](https://doi.org/10.1038/srep23114), Publisher: Nature Publishing Group.
- [26] K.-V. Pham, *Internal spin resistance of spin batteries*, doi:[10.48550/arXiv.1803.07101](https://doi.org/10.48550/arXiv.1803.07101), ArXiv:1803.07101 [cond-mat] (2018).
- [27] K.-V. Pham, *Infinite magnetoresistive effect in spin valves* (2024).
- [28] J. Bass and W. P. Pratt, *Current-perpendicular (CPP) magnetoresistance in magnetic metallic multilayers*, Journal of Magnetism and Magnetic Materials **200**(1), 274 (1999), doi:[10.1016/S0304-8853\(99\)00316-9](https://doi.org/10.1016/S0304-8853(99)00316-9).
- [29] J. C. Slonczewski, *Conductance and exchange coupling of two ferromagnets separated by a tunneling barrier*, Physical Review B **39**(10), 6995 (1989), doi:[10.1103/PhysRevB.39.6995](https://doi.org/10.1103/PhysRevB.39.6995).
- [30] J. S. Moodera, L. R. Kinder, T. M. Wong and R. Meservey, *Large Magnetoresistance at Room Temperature in Ferromagnetic Thin Film Tunnel Junctions*, Physical Review Letters **74**(16), 3273 (1995), doi:[10.1103/PhysRevLett.74.3273](https://doi.org/10.1103/PhysRevLett.74.3273), Publisher: American Physical Society.
- [31] J. Bass, *CPP magnetoresistance of magnetic multilayers: A critical review*, Journal of Magnetism and Magnetic Materials **408**, 244 (2016), doi:[10.1016/j.jmmm.2015.12.011](https://doi.org/10.1016/j.jmmm.2015.12.011).

- [32] J. Bass and W. P. Pratt, *Spin-diffusion lengths in metals and alloys, and spin-flipping at metal/metal interfaces: an experimentalist's critical review*, *Journal of Physics: Condensed Matter* **19**, 183201 (2007), doi:[10.1088/0953-8984/19/18/183201](https://doi.org/10.1088/0953-8984/19/18/183201).
- [33] S. Yuasa, T. Nagahama, A. Fukushima, Y. Suzuki and K. Ando, *Giant room-temperature magnetoresistance in single-crystal Fe/MgO/Fe magnetic tunnel junctions*, *Nature Materials* **3**(12), 868 (2004), doi:[10.1038/nmat1257](https://doi.org/10.1038/nmat1257), Publisher: Nature Publishing Group.